The Cryosphere Discuss., 9, 4377–4405, 2015
www.the-cryosphere-discuss.net/9/4377/2015/
doi:10.5194/tcd-9-4377-2015

The Cryosphere Discussions
Open Access

Orographic and vegetation effects on snow accumulation in the southern Sierra Nevada: a statistical summary from LiDAR data

Z. Zheng[1], **P. B. Kirchner**[2,3], **and R. C. Bales**[1,4]

[1]Department of Civil and Environmental Engineering, UC Berkeley, Berkeley, CA, USA
[2]Joint Institute for Regional Earth System Science and Engineering, Pasadena, CA, USA
[3]Southwest Alaska Network, National Park Service, Anchorage, AK, USA
[4]Sierra Nevada Research Institute, UC Merced, Merced, CA, USA

Received: 20 July 2015 – Accepted: 23 July 2015 – Published: 19 August 2015

Correspondence to: Z. Zheng (zeshi.z@berkeley.edu)

Published by Copernicus Publications on behalf of the European Geosciences Union.

Abstract

Airborne light detection and ranging (LiDAR) snow-on and snow-off measurements collected in the southern Sierra Nevada in the 2013 water year were analyzed for orographic and vegetation effects on snow accumulation during the winter season. Combining data from four sites separated by 10 to 64 km and together covering over 106 km^2 area, the 1 m elevation-band-averaged snow depth in canopy gaps as a function of elevation increased at a rate of 15 cm per 100 m until reaching the elevation of 3300 m. The averaged snow depth of the same elevation band from different sites matched up with minor deviation, which could be partially attributed to the variation in other topographic features, such as slope and aspect. As vegetation plays a role in the snow accumulation, the distribution of the vegetation was also studied and shows that the canopy coverage consistently decreased along the elevation gradient from 80 % at 1500 m to near 0 % at above 3300 m. Also, the absolute difference of the averaged snow depth between snow found in canopy gaps and under the canopy increased with elevation, and decreased with canopy coverage disregarding the variation of other topographic features. The influence from the forest density on snow accumulation was quantified based on the snow-depth residuals from 1 m elevation-band-averaged snow depth and the attribute penetration fraction, which is the ratio of the number of ground points to the number of total points per pixel of LiDAR data. The residual increases from −25 to 25 cm at the penetration fraction range of 0 to 80 %; and the relationship could be modeled by exponential functions, with minor fluctuations along the gradient fraction of canopy and small deviation between sites.

1 Introduction

In the western United States, mountain snowpack is the primary source of late-spring and early summer streamflow and is associated with agricultural and municipal water supplies (Bales et al., 2006). Knowledge of spring snowpack conditions within a water-

shed is essential if water availability and flood peaks following the onset of melt are to be accurately predicted (Hopkinson et al., 2001). Both topographic and vegetation factors are important in influencing the snowpack conditions, as they closely interact with meteorological conditions to affect precipitation and snow accumulation distribution in the mountains (McMillen, 1988; Raupach, 1991; Wigmosta et al., 1994). However, the distribution of mountain precipitation is poorly understood at multiple spatial scales because it is governed by processes that are neither well measured nor accurately predicted (Kirchner et al., 2014). Snow accumulation across the mountains is primarily influenced by orographic processes, involving feedbacks between atmospheric circulation and terrain (Roe, 2005; Roe and Baker, 2006). In forested regions snow accumulation is highly sensitive to vegetation structure (Anderson, 1963; Revuelto et al., 2015; Musselman et al., 2008), and canopy snow interception, sublimation and unloading results in smaller accumulations of snow beneath the forest canopies in comparison with canopy gaps (Mahat and Tarboton, 2013).

The Sierra Nevada serves as a barrier to moisture moving inland from the Pacific, provides an ideal mountainous region for producing orographic precipitation, and exerts a strong influence on the upslope amplification of precipitation (Colle, 2004; Rotach and Zardi, 2007; Smith and Barstad, 2004). And among the forested regions of the mountains, the mixed-conifer and subalpine zones cover most of the high-elevation area. The geographic, topographic, and vegetation conditions make the Sierra Nevada a natural laboratory in the western United States for studying mountain snow distribution and related hydrologic processes (Grünewald et al., 2013, 2014; Lehning et al., 2011).

In order to have a better knowledge of precipitation and snow accumulation in the Sierra Nevada, manual snow surveys, one-time surveys, and remote-sensing products are used and analyzed (Guan et al., 2013). In situ observations of snow water equivalent (SWE) were obtained from monthly manual snow surveys and daily snow pillow observations (Rosenberg et al., 2011). Cost, data coverage, accuracy (Julander et al., 1998) and basin-scale representativeness are issues for in situ monitoring of

SWE in mountainous terrain (Rice and Bales, 2010). Satellite-based remote sensing, such as MODIS, has been used to map snow coverage in large or even global areas. Fractional snow coverage, grain size and albedo have retrieved from MODIS data (Hall et al., 2002; Painter et al., 2009; Rittger et al., 2013), however the products do not fit catchment-size studies owing to its low spatial resolution. It also only provides snow-coverage information in canopy gaps, and no direct information on snow depths. There is also SNOw Data Assimilation Systems (SNODAS) that integrate data from satellite and in situ measurements into physical snowpack model, which provides SWE and snow depth information (Barrett, 2003). Since the spatial resolution of SNODAS is 1 km and its products have not been globally evaluated (Clow et al., 2012), SNODAS could not be used for studying the snow distribution on catchment scale in the Sierra Nevada.

In recent years, airborne LiDAR has been employed for high-spatial-resolution distance measurements (Hopkinson et al., 2004), and has become an important technique to acquire topographic data with sub-meter resolution and accuracy (Marks and Bates, 2000). Therefore, LiDAR provides a potential tool to help understand spatially distributed snow depth across mountainous regions. With multiple returns from a single laser beam, LiDAR has also been used to construct vegetation structures as well as observe conditions under the canopy, which helps produce fine-resolution DEMs, vegetation structures, and snow-depth information.

Even without LiDAR surveys, Erickson et al. (2005) and Erxleben et al. (2002) have used intensive in situ SWE measurements with binary regression tree, linear and nonlinear multivariate regression models for studying the topographic and vegetation controls on the spatial distribution of snow in the Colorado Rocky Mountains. But the studying sites were smaller than catchment size, and the results were site dependent as well as the sampling schemes have to be taken into consideration. Recent snow distribution modeling methods developed upon LiDAR measurements have been focused on fractal analysis and linear regression. Even the fractal distributions of snow depth do not vary with sites on local scale from 1 to 1000 m (Deems et al., 2006) and the topo-

graphic dependency of spatial snow-depth distribution have been explored (Kirchner et al., 2014), consistency of the topographic and vegetation effects across sites still need to be addressed.

The objective of this work is to improve our understanding of the effect of elevation, slope, aspect and canopy cover on snow accumulation. We investigate these by using LiDAR data collected in four headwater catchments in the southern Sierra Nevada and address the following three questions. First, is there a consistent orographic effect on snow accumulation across catchments; and what attributes could account for variability across and within sites? Second, what is the snow-depth difference between canopy gaps, vs. under canopy, along elevation; and is binary classification for canopy cover adequate to the differences? Third, how does forest density influence the snow accumulation in canopy gaps and if there are patterns, are they consistent across catchments?

2 Methods

2.1 Study areas

The study area is located in the southern Sierra Nevada, 80 km east of Fresno, California (Fig. 1). Four headwater-catchment research areas, Bull Creek, Shorthair Creek, Providence Creek, and Wolverton Basin were previously instrumented, including meteorological measurements, in order to have a better knowledge of the hydrological processes in this region (Bales et al., 2011; Hunsaker et al., 2012; Kirchner et al., 2014). Wolverton is approximately 64 km away in the southeast direction of the other three sites (Fig. 1) and is located in Sequoia National Park. Both snow-on and snow-off airborne LiDAR were flown in 2010 (Table 1, only later date collections were processed) over these sites. The elevation of the survey areas covers from 1600 to 3500 m elevation, over which vegetation density generally decreases with biotic zones of subalpine forest and a large area above treeline in Wolverton (Goulden et al., 2012). The precipitation has historically been mostly snow in the cold and wet winters for elevations above 2000 m, and rain-snow transition below 2000 m.

2.2 Data collection

Both airborne LiDAR surveys were performed by using Optech GEMINI Airborne Laser Terrain Mapper. The scan angle and scan frequency were adjusted to ensure a uniform along-track and across-track point spacing (Table 2), and six GPS ground stations were used for determining aircraft trajectory. The snow-on survey date was close to 1 April, which is used by operational agencies as peak snow time. Since the snow-on survey lasted four days to finish data collection over the four study areas, time-series in situ snow-depth data measured continuously from Judd Communications ultrasonic depth sensors of the meteorological stations at Providence, Bull and Wolverton were used for checking if precipitation had occurred during survey dates and also taking snowpack densification and melting into considerations (Hunsaker et al., 2012; Kirchner et al., 2014). The snow-off survey was performed in August when snow was completely melted out in the study areas.

2.3 Data processing

Raw LiDAR datasets were pre-processed by NCALM and available from the NSF Open-Topography website (http://opentopography.org) in LAS format. The LAS point clouds, both canopy and ground-surface points, are stored and classified as ground return and vegetation return; each point is also attributed with the total number of returns and position of all returns from its source laser beam. The 1 m resolution digital-elevation models, generated from the LiDAR point-cloud datasets, were downloaded from the OpenTopography database and further processed in ArcMap 10.2 to generate 1 m resolution slope, aspect, and northness raster products. Northness is an index for the potential amount of solar radiation reaching a slope on a scale of −1 to 1, calculated from:

$$N = \sin(S) \times \cos(A), \quad (1)$$

where N is the northness value; S is the slope angle of the terrain; and A is the aspect angle. Northness is also the same as the aspect intensity (Kirchner et al., 2014) with 0° focal aspect. Since in this analysis snow-depth comparison is only discussed between north and south facing slopes, northness is used instead of aspect intensity for simplification. To construct the vegetation structure from LiDAR data, points that are from the first return of the laser beam are used to generate 1 m gridded digital surface model. A 1 m resolution canopy-height model was built by subtracting the digital-elevation model from the digital-surface model.

The snow depths were calculated directly from the snow-on LiDAR data. By referring to canopy-height models, all ground points in snow-on LiDAR datasets were classified as under canopy or in canopy gaps. That is, if the point was under canopy of > 2 m height, it was classified as under canopy, and otherwise in a canopy gap. After classification, snow depths were calculated by subtracting the values in the digital-elevation model from the snow-on point-measurement values. The calculated point snow-depth data were further assigned into 1 m raster pixels, averaged within each pixel, formatted and then gap filled by interpolation with pixel values around it. Since the measurements collected under canopy were insufficient within each pixel (Fig. 2) and varied across the transition from the tree trunk to the edge of the canopy, interpolation was not applied to data under the canopy.

2.4 Penetration fraction

Open-canopy fraction is a factor that represents the forest density above a given pixel and is often used to describe the influence of vegetation on snow accumulation and melt. However there is no algorithm to directly extract this information from LiDAR data. Here we use a novel approach we call penetration fraction to approximate the open-canopy fraction from the LiDAR point cloud. Penetration fraction is the ratio of

the number of ground points and number of received laser beams within each pixel (Fig. 3). Because both the LiDAR and sunlight beams are intercepted by canopies, the open-canopy fraction is oftenly used here as an index to represent the fraction of sunlight radiance received on the ground under vegetation. Therefore, penetration fraction of LiDAR is actually another form of the open-canopy fraction estimation. However, under-canopy vegetation can also intercept the LiDAR beam causing a bias. To eliminate this bias, the canopy-height model was used to check if the pixel was canopy covered; and if not, the local penetration fraction of the pixel was reset to 1 because the open-canopy fraction of a pixel could not be entirely represented by the penetration fraction. A spatial moving-average process was applied using a 2-D Gaussian filter with a radius of 5 m to account for the effect of the vegetation around each pixel.

2.5 Statistical analysis

Using elevation, slope, aspect, vegetation-structure and snow-depth retrieved from LiDAR measurements, orographic and vegetation effects on snowpack accumulation were analyzed statistically. Owing to orographic effects, there is increasing precipitation along an increasing elevation gradient in this area (Kirchner et al., 2014). Therefore, elevation was selected as the primary topographic attribute. All snow-depth measurements from LiDAR were first separated by either under canopy or in canopy gaps, and then were binned by elevation of the location where they were measured, with a bin size of 1 m elevation. As each elevation band had hundreds of snow-depth measurements after binning, the average of all snow depths was chosen as the representative snow depth, and the standard deviation calculated to represent the snow-depth variability within each elevation band. Correlation coefficients between snow depth and elevation of each site were calculated by linear regression. Northness and slope were also averaged by elevation band for cross comparison. The differences of averaged snow depth between in canopy gaps and under-canopy areas were calculated for each elevation band and cross compared with the vegetation fraction, northness and slope.

To account for effects other than elevation in the snow depth, a linear regression model of snow depth and elevation was applied to the digital-elevation data to estimate snow depth. The differences between the estimated and LiDAR-measured snow depths were further investigated, with respect to slope, aspect and penetration fraction, by binning the snow-depth difference into 1° slope and aspect bins and 1 % penetration-fraction bins. The difference values within each bin were averaged and the standard deviations were calculated.

3 Results

The snow depth estimated in canopy gaps shows a strong consistency of distribution patterns and variability across the four sites (Fig. 4a and b). In general, snow depth is linearly correlated with elevation at all sites, both in the open area and under the canopy, snow depth under the canopy is consistently less than in the canopy gaps (Fig. 5a). Note that values at the upper or lower ends of elevation at each site have few pixels and maybe less representative of the values of physiographic attributes in the study areas (Fig. 4c). The forested area, of all four sites combined, spans the rain-snow transition zone in mixed conifer through subalpine forest to significant areas above treeline. The snow-depth difference between canopy gaps and under-canopy varies with elevation, generally increasing from near zero at 1500 m, where there is little snow but dense canopy, to 40 cm in the range of 2000–2400 m, and varying from near zero to 60 cm at higher elevation where snow is deeper and canopy less dense.

For each individual site, the least-squares linear regressions of snow depth and elevation were used to investigate the spatial variability of snow-depth across sites. The elevation of the three sites increases in going from Providence to Bull to Shorthair. Providence Creek goes down to 1400 m, and snow depth increases steeply in this region at a rate of 38 cm per 100 m in canopy gaps and 28 cm per 100 m under the canopy. Bull Creek has an elevation range of 2000–2400 m, which is slightly higher than Providence, and has snow depth increasing at 21 cm per 100 m in canopy gaps

and 19 cm per 100 m under the canopy. For Shorthair Creek site, which is the highest of the three, the snow depth increases at 17 cm per 100 m in canopy gaps and 16 cm per 100 m under the canopy. Wolverton is 64 km further south and spans a wide elevation range, going from the rain-snow transition in mixed conifer, to subalpine forest, to some area above treeline. The average snow-depth increase is smallest among all four study sites, 15 cm per 100 m in canopy gaps and 13 cm per 100 m under the canopy. Unlike the other three lower-elevation sites, the snow depth at Wolverton site decreases after 3300 m elevation. However, the amount of area above this elevation also drops off steeply.

A visual inspection of the pattern of snowpack distribution with elevation for all sites shows a consistent pattern (Fig. 4). Especially for the elevation range where Providence and Wolverton overlap, the patterns of snow depth change are the same for both sites, with the only difference being Wolverton snow depth is consistently less than that in Providence, which is likely due to a small amount of densification that occurred between the two acquisitions (Table 1) observed from depth sensors.

At higher elevations, vegetation coverage decreases consistent with lower temperature, and soil depth. By cross comparing the vegetation fraction and snow-depth difference (Fig. 5a and b), similar patterns were observed at all sites along elevation gradient. Also, for most of the elevation range investigated, the snow-depth difference was either increasing or remaining constant, except for 2300 to 2500 m at Wolverton, where the snow-depth difference drops drastically, which may be explained by steeper and more southerly exposed slopes (Kirchner et al., 2014) (Fig. 6).

The snow-depth residual deviation from a linear increase with elevation, investigated vs. penetration fraction (Fig. 7), indicates how the density of vegetation affects the snow-depth accumulation in canopy gaps. For all sites, the snow-depth residuals increase with penetration fraction, with bias across sites and fluctuations at higher penetration fractions.

4 Discussion

The overall increasing trend of precipitation with elevation observed from airborne LiDAR data is consistent with the orographic effect on precipitation (Roe, 2005; Roe and Baker, 2006) and less snow accumulation was observed under vegetation at all sites. The decrease in under-canopy snow is consistent with previous work using ground-based data (Bales et al., 2011; Musselman et al., 2008; Varhola et al., 2010). Finally, the penetration fraction explained part of the snow-depth residual of the linear model between snow depth and elevation.

4.1 Orographic effect on snow accumulation

Below 3300 m, the increasing trend of snow accumulation with elevation was observed for all sites (Fig. 4). Linear regression is applicable to model the relationship between snow depth and elevation when the study area has a broad elevation range. As indicated in Table 3, the correlation coefficient of linear model used for Shorthair site is much smaller than the other three sites. The other three sites all have elevation range larger than 500 m; however the elevation spans around 200 m at Shorthair site. The bias of mean snow depth in the same elevation band between different sites is acceptable if the standard error is being added or subtracted from the mean (Fig. 4a and b). The data-collection time, spatial variation and variations of other topographic features should introduce bias across sites. However, as data-collection time only differs a few days in situ snow-depth sensor data suggest that the melting and densification effect should be under 2 cm (https://czo.ucmerced.edu/dataCatalog_sierra.html). Spatial variations at 1800–2000 m elevations between Providence and the further south Wolverton site appear to have a consistent bias, with less precipitation falling in the southerly location. For other topographic features, Kirchner et al. (2014) proposed that northness and slope should have negative effects on snow accumulation. They noted that northness is positively correlated with solar radiation, and thus ablation, and northeastness deposition from prevailing winds. Steeper slopes also have has higher avalanche po-

tential and snow is more likely to fall off from these slopes. Across the elevation range that we studied, the snow depth is globally smaller at Wolverton than all other sites; however the northness and slope are globally higher at Wolverton, which is consistent with the northness and slope effects on snow accumulation. Also, the separate investigations on slope and aspect (Fig. 6) show that smaller snow-depth residuals could be observed on steeper or more southerly exposed slopes, which further proved the existence of the northness effect. From Fig. 2 we also need to notice that each site has about 10 to 24 % of total surveyed area does not have point return because of canopy interception. Thus the statistical results are representative but not conclusive of surveyed sites.

4.2 Vegetation effects on snow accumulation along elevation

The snow depth in open areas is increasing 2 cm/100 m to 12 cm/100 m steeper than snow depth in under-canopy areas (Table 3). Schmidt and Gluns (1991) found that the snow intercepted by canopy increases with cumulative snowfall and the interception would saturate when the precipitation is heavy enough. Therefore, in our study sites, with more snow intercepted at higher elevation, the snow-depth increasing slope of under-canopy observations is gentler than open areas.

The difference of averaged snow depth between open and under-canopy areas increases with elevation as vegetation coverage decreases (Fig. 5a and b). We found that a high density of vegetation exerts a negative influence on snow accumulation in canopy gaps, which makes the snow-depth difference less significant at lower elevations. With precipitation increasing along the elevation gradient, the difference of snow depth between open and canopy-covered areas also increases; and in more densely forested areas, even though the open area does not have canopy right above the ground (Hedstrom and Pomeroy, 1998; Pomeroy et al., 2002; Schmidt and Gluns, 1991) they can still be influenced by the canopies around them. Golding and Swanson (1986) found that the difference increased with clearing size, caused by snow ablation as well as direct solar radiation reaching the snowpack. Another cause of this effect

could be traced back to how precipitation drops on the ground. As precipitation has both horizontal and vertical velocities, in a densely forested area a small fraction of snowflakes or raindrops would be intercepted by the vegetation, not only vertically, but also horizontally. Therefore, the snow accumulated in the open area that is surrounded by dense vegetation would actually be smaller than the snow accumulated in a wide-open area. This is also consistent with the finding that areas at the drip edge have snow-depth values, intermediate between under canopy and in the open (Bales et al., 2011). Thus in the more-open forests at higher elevation, the under-canopy and in-canopy-gap allow for greater snow-depth differences. Since the differences could change in different forest conditions and also under the effect of drip-edge transitions, binary classification of in canopy gaps and under-canopy does not work for quantifying differences in snow accumulation.

Furthermore, the pattern could be altered as some other topographic feature varies. We observed a sudden drop of snow-depth difference in the elevation range of 2300–2500 m at Wolverton from Fig. 5a. By visually inspecting the vegetation-pixel percentage, northness, and slope along the elevation gradient (Figs. 4d and 5b and c), it is observed that the vegetation pixel percentage decreases constantly at a low rate and northness decreases from positive to negative (north dominant to south dominant); while the slope kept increasing significantly in this elevation range. Dubayah (1994), Courbaud et al. (2003), and Essery et al. (2008) found that slope is a dominant factor in modeling the solar radiation received by the soil when canopy structures remain constant, and more solar radiation would be received on steeper south facing slopes, which could be the cause of the snow-depth difference decrease that we observed.

4.3 Quantify vegetation effects on snow accumulation

In the previous section, we reasoned that vegetation reduces snow accumulation in canopy gaps by blocking the snow that in a less-dense forest would fall to the ground. Vegetation density is a significant factor (Teti, 2003), as we observed that snow-depth difference increases when vegetation fraction decreases. Figure 7 shows the quantification of the vegetation-density effects on the snow-depth accumulation. Considering the blocking of snow from vegetation (Pomeroy et al., 1998; Schmidt and Gluns, 1991), the vegetation density should be transformed into open fraction that one could see from the given pixel. In this case, penetration fraction was applied to represent percentage opening. As is shown in Fig. 7a, the snow-depth residual differed from the linear increase with elevation is highly correlated with penetration fraction, which implies that penetration fraction is a good indicator of vegetation effects on snow accumulation. Moreover, the ranges of the snow-depth residual are similar and the patterns of snow-depth residual changing against penetration fraction are consistent across sites, as the studied sites share similar vegetation structures and climate conditions (Fites-Kaufman et al., 1970). The consistency of changing patterns supports the idea of modeling the relationship between vegetation density and snow depth so that the effects from vegetation on open area snow accumulation could be quantified.

5 Conclusions

The regression analysis of snow depth vs. terrain and vegetation attributes that are extracted from LiDAR show that snow accumulation in the southern Sierra Nevada is strongly affected by both the orographic effect and vegetation factors, and are consistent across the four sites studied. Comparing these results across sites reveals that the altitudinal effects on snow accumulation are consistent and globally linear, with a lapse rate of approximately 15 cm per 100 m. By cross comparing between snow depth and other topographic features along the elevation gradient, we confirmed that the variability of snow depth, after de-trending the altitudinal effect, could be further explained by attributes such as slope and aspect. The characterization of snow-depth difference between open and canopy-covered area, together with vegetation fraction, not only suggests that the snow-depth-difference increase along the elevation gradient is because of vegetation density decreasing, it also suggests that, penetration fraction can be used to quantitatively study vegetation effects on snow accumulation. Moreover, the

analysis of the snow-depth residual from the altitudinal trend and penetration fraction reveals that the vegetation effects on snow accumulation are consistent across the four study-sites, implying that the effects could be quantified and modeled mathematically.

Acknowledgements. This material is based on data and processing services provided by the OpenTopograhy Facility with support from the National Science Foundation under NSF Award Numbers 1226353 and 1225810. Research was supported by the National Science Foundation under NSF Award Numbers 1331939 and 1239521. We acknowledge the helpful comments from Q. Guo, A. Harpold, and N. P. Molotch, also Q. Guo and J. Flanagan for providing canopy height model data.

References

Anderson, H. W.: Managing California's Snow Zone Lands for Water, Pacific Southwest For. Range Exp. Station, Berkeley, CA, 1963.

Bales, R. C., Molotch, N. P., Painter, T. H., Dettinger, M. D., Rice, R., and Dozier, J.: Mountain hydrology of the western United States, Water Resour. Res., 42, W08432, doi:10.1029/2005WR004387, 2006.

Bales, R. C., Hopmans, J. W., O'Geen, A. T., Meadows, M., Hartsough, P. C., Kirchner, P., Hunsaker, C. T., and Beaudette, D.: Soil moisture response to snowmelt and rainfall in a Sierra Nevada mixed-conifer forest, Vadose Zone J., 10, 786–799, doi:10.2136/vzj2011.0001, 2011.

Barrett, A. P.: National operational hydrologic remote sensing center SNOw data assimilation system (SNODAS) products at NSIDC, NSIDC Spec. Rep. 11, Natl. Snow and Ice Data Cent., Boulder, CO, 2003.

Clow, D. W., Nanus, L., Verdin, K. L., and Schmidt, J.: Evaluation of SNODAS snow depth and snow water equivalent estimates for the Colorado Rocky Mountains, USA, Hydrol. Process., 26, 2583–2591, doi:10.1002/hyp.9385, 2012.

Colle, B. A.: Sensitivity of orographic precipitation to changing ambient conditions and terrain geometries: an idealized modeling perspective, J. Atmos. Sci., 61, 588–606, doi:10.1175/1520-0469(2004)061<0588:SOOPTC>2.0.CO;2, 2004.

Courbaud, B., De Coligny, F., and Cordonnier, T.: Simulating radiation distribution in a heterogeneous Norway spruce forest on a slope, Agr. Forest Meteorol., 116, 1–18, doi:10.1016/S0168-1923(02)00254-X, 2003.

Deems, J. S., Fassnacht, S. R., and Elder, K. J.: Fractal distribution of snow depth from lidar data, J. Hydrometeorol., 7, 285–297, doi:10.1175/JHM487.1, 2006.

Dubayah, R. C.: Modeling a solar radiation topoclimatology for the Rio Grande River Basin, J. Veg. Sci., 5, 627–640, doi:10.2307/3235879, 1994.

Erickson, T. A., Williams, M. W., and Winstral, A.: Persistence of topographic controls on the spatial distribution of snow in rugged mountain terrain, Colorado, United States, Water Resour. Res., 41, 1–17, doi:10.1029/2003WR002973, 2005.

Erxleben, J., Elder, K., and Davis, R.: Comparison of spatial interpolation methods for estimating snow distribution in the Colorado Rocky Mountains, Hydrol. Process., 16, 3627–3649, doi:10.1002/hyp.1239, 2002.

Essery, R., Bunting, P., Rowlands, A., Rutter, N., Hardy, J., Melloh, R., Link, T., Marks, D., and Pomeroy, J.: Radiative transfer modeling of a coniferous canopy characterized by airborne remote sensing, J. Hydrometeorol., 9, 228–241, doi:10.1175/2007JHM870.1, 2008.

Fites-Kaufman, J., Rundel, P., Stephenson, N., and Weixelman, D. A.: Montane and subalpine vegetation of the Sierra Nevada and Cascade Ranges, Terr. Veg. Calif., 17, 456–501, 1970.

Golding, D. L. and Swanson, R. H.: Snow distribution patterns in clearings and adjacent forest, Water Resour. Res., 22, 1931, doi:10.1029/WR022i013p01931, 1986.

Goulden, M. L., Anderson, R. G., Bales, R. C., Kelly, A. E., Meadows, M., and Winston, G. C.: Evapotranspiration along an elevation gradient in California's Sierra Nevada, J. Geophys. Res.-Biogeo., 117, 1–13, doi:10.1029/2012JG002027, 2012.

Grünewald, T., Stötter, J., Pomeroy, J. W., Dadic, R., Moreno Baños, I., Marturià, J., Spross, M., Hopkinson, C., Burlando, P., and Lehning, M.: Statistical modelling of the snow depth distribution in open alpine terrain, Hydrol. Earth Syst. Sci., 17, 3005–3021, doi:10.5194/hess-17-3005-2013, 2013.

Grünewald, T., Bühler, Y., and Lehning, M.: Elevation dependency of mountain snow depth, The Cryosphere, 8, 2381–2394, doi:10.5194/tc-8-2381-2014, 2014.

Guan, B., Molotch, N. P., Waliser, D. E., Jepsen, S. M., Painter, T. H., and Dozier, J.: Snow water equivalent in the Sierra Nevada: blending snow sensor observations with snowmelt model simulations, Water Resour. Res., 49, 5029–5046, doi:10.1002/wrcr.20387, 2013.

Hall, D. K., Riggs, G. A., Salomonson, V. V., DiGirolamo, N. E., and Bayr, K. J.: MODIS snow-cover products, Remote Sens. Environ., 83, 181–194, doi:10.1016/S0034-4257(02)00095-0, 2002.

Hedstrom, N. R. and Pomeroy, J. W.: Measurements and modelling of snow interception in the boreal forest, Hydrol. Process., 12, 1611–1625, doi:10.1002/(SICI)1099-1085(199808/09)12:10/11<1611::AID-HYP684>3.0.CO;2-4, 1998.

Hopkinson, C., Sitar, M., Chasmer, L., Gynan, C., Agro, D., Enter, R., Foster, J., Heels, N., Hoffman, C., Nillson, J., and St. ierre, R.: Mapping the spatial distribution of snowpack depth beneath a variable forest canopy using airborne laser altimetry, in: Proc. 58th Annu. East. Snow Conf., Ottawa, Ontario, Canada, 2001.

Hopkinson, C., Sitar, M., Chasmer, L., and Treitz, P.: Mapping snowpack depth beneath forest canopies using airborne lidar, Photogramm. Eng. Rem. S., 70, 323–330, 2004.

Hunsaker, C. T., Whitaker, T. W., and Bales, R. C.: Snowmelt runoff and water yield along elevation and temperature gradients in California's Southern Sierra Nevada1, J. Am. Water Resour. As., 48, 667–678, doi:10.1111/j.1752-1688.2012.00641.x, 2012.

Kirchner, P. B., Bales, R. C., Molotch, N. P., Flanagan, J., and Guo, Q.: LiDAR measurement of seasonal snow accumulation along an elevation gradient in the southern Sierra Nevada, California, Hydrol. Earth Syst. Sci., 18, 4261–4275, doi:10.5194/hess-18-4261-2014, 2014.

Lehning, M., Grünewald, T., and Schirmer, M.: Mountain snow distribution governed by an altitudinal gradient and terrain roughness, Geophys. Res. Lett., 38, 1–5, doi:10.1029/2011GL048927, 2011.

Mahat, V. and Tarboton, D. G.: Representation of canopy snow interception, unloading and melt in a parsimonious snowmelt model, Hydrol. Process., 28, 6320–6336, doi:10.1002/hyp.10116, 2013.

Marks, K. and Bates, P.: Integration of high-resolution topographic data with floodplain flow models, Hydrol. Process., 14, 2109–2122, doi:10.1002/1099-1085(20000815/30)14:11/12<2109::AID-HYP58>3.0.CO;2-1, 2000.

McMillen, R. T.: An eddy correlation technique with extended applicability to non-simple terrain, Bound.-Lay. Meteorol., 43, 231–245, doi:10.1007/BF00128405, 1988.

Musselman, K. N., Molotch, N. P., and Brooks, P. D.: Effects of vegetation on snow accumulation and ablation in a mid-latitude sub-alpine forest, Hydrol. Process., 22, 2767–2776, doi:10.1002/hyp.7050, 2008.

Painter, T. H., Rittger, K., McKenzie, C., Slaughter, P., Davis, R. E., and Dozier, J.: Retrieval of subpixel snow covered area, grain size, and albedo from MODIS, Remote Sens. Environ., 113, 868–879, doi:10.1016/j.rse.2009.01.001, 2009.

Pomeroy, J. W., Parviainen, J., Hedstrom, N., and Gray, D. M.: Coupled modelling of forest snow interception and sublimation, Hydrol. Process., 12, 2317–2337, doi:10.1002/(SICI)1099-1085(199812)12:15<2317::AID-HYP799>3.0.CO;2-X, 1998.

Pomeroy, J. W., Gray, D. M., Hedstrom, N. R., and Janowicz, J. R.: Prediction of seasonal snow accumulation in cold climate forests, Hydrol. Process., 16, 3543–3558, doi:10.1002/hyp.1228, 2002.

Raupach, M. R.: Vegetation-atmosphere interaction in homogeneous and heterogeneous terrain: some implications of mixed-layer dynamics, Vegetatio, 91, 105–120, doi:10.1007/BF00036051, 1991.

Revuelto, J., Lopez-Moreno, J. I., Azorin-Molina, C., and Vicente-Serrano, S. M.: Canopy influence on snow depth distribution in a pine stand determined from terrestrial laser data, Water Resour. Res., 51, 3476–3489, doi:10.1002/2014WR016496, 2015.

Rice, R. and Bales, R. C.: Embedded-sensor network design for snow cover measurements around snow pillow and snow course sites in the Sierra Nevada of California, Water Resour. Res., 46, 1–13, doi:10.1029/2008WR007318, 2010.

Rittger, K., Painter, T. H., and Dozier, J.: Assessment of methods for mapping snow cover from MODIS, Adv. Water Resour., 51, 367–380, doi:10.1016/j.advwatres.2012.03.002, 2013.

Roe, G. H.: Orographic precipitation, Annu. Rev. Earth Pl. Sc., 33, 645–671, doi:10.1146/annurev.earth.33.092203.122541, 2005.

Roe, G. H. and Baker, M. B.: Microphysical and geometrical controls on the pattern of orographic precipitation, J. Atmos. Sci., 63, 861–880, doi:10.1175/JAS3619.1, 2006.

Rosenberg, E. A., Wood, A. W., and Steinemann, A. C.: Statistical applications of physically based hydrologic models to seasonal streamflow forecasts, Water Resour. Res., 47, W00H14, doi:10.1029/2010WR010101, 2011.

Rotach, M. W. and Zardi, D.: On the boundary-layer structure over highly complex terrain: key findings from MAP, Q. J. Roy. Meteorol. Soc., 133, 937–948, doi:10.1002/qj.71, 2007.

Schmidt, R. A. and Gluns, D. R.: Snowfall interception on branches of three conifer species, Can. J. Forest Res., 21, 1262–1269, doi:10.1139/x91-176, 1991.

Smith, R. B. and Barstad, I.: A linear theory of orographic precipitation, J. Atmos. Sci., 61, 1377–1391, doi:10.1175/1520-0469(2004)061<1377:ALTOOP>2.0.CO;2, 2004.

Teti, P.: Relations between peak snow accumulation and canopy density, Forest. Chron., 79, 307–312, 2003.
Varhola, A., Coops, N. C., Weiler, M., and Moore, R. D.: Forest canopy effects on snow accumulation and ablation: an integrative review of empirical results, J. Hydrol., 392, 219–233, doi:10.1016/j.jhydrol.2010.08.009, 2010.
Wigmosta, M. S., Vail, L. W., and Lettenmaier, D. P.: A distributed hydrology-vegetation model for complex terrain, Water Resour. Res., 30, 1665–1680, doi:10.1029/94WR00436, 1994.

Table 1. LiDAR data collection information, later date data were used for analyses in this paper.

	Snow-off flight date	Snow-on flight date	Area, km^2
Bull	15 August 2010	24 March 2010	22.3
Shorthair	13 August 2010	15 March 2010 23 March 2010	6.8
Providence	5 August 2010	15 March 2010 23 March 2010	18.4
Wolverton	13–15 August 2010	21–22 March 2010	58.9

Table 2. Flight parameters and sensor settings.

Flight parameters		Equipment settings	
flight altitude	600 m	wavelength	1047 nm
flight speed	65 m s^{-1}	beam divergence	0.25 mrad
swath width	233.26 m	laser PRF	100 kHz
swath overlap	50 %	scan frequency	55 Hz
point density	10.27 p m^{-2}	scan angle	±14°
Cross track res	0.233 m	scan cutoff	3°
Down track res	0.418 m	scan offset	0°

Table 3. Linear regression of snow depth vs. elevation in four sites.

	Bull	Shorthair	Providence	Wolverton
Open R^2	0.968	0.797	0.931	0.914
Vegetated R^2	0.978	0.737	0.921	0.972
Open slope, cm 100 m^{-1}	21.6	16.1	37.8	15.3
Vegetated slope, cm 100 m^{-1}	19.9	13.1	26.0	13.4

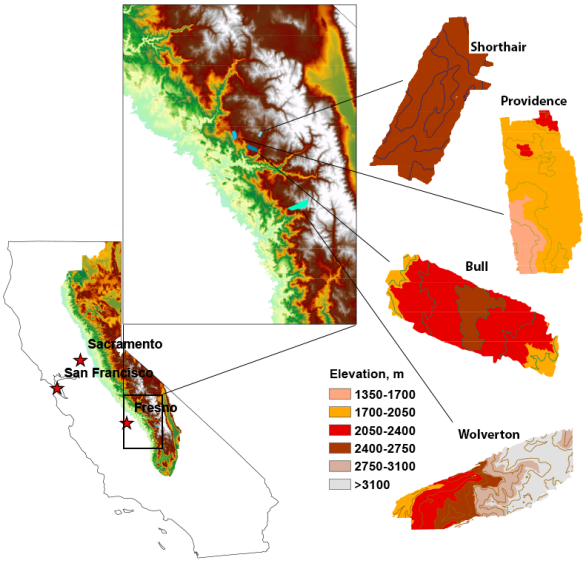

Figure 1. Study area and LiDAR footprints. (Left) California with Sierra Nevada. (Center) Zoomed view to show the locations of LiDAR footprints. (Right) Elevation and 200 m contour map (100 m for Bull) of LiDAR footprints.

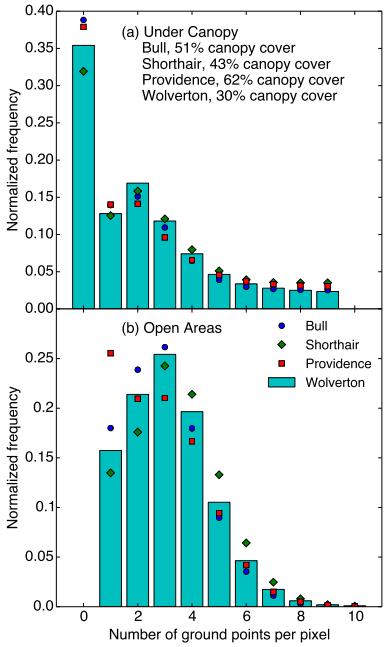

Figure 2. (a) Normalized histogram of the number of ground points for under canopy pixels. **(b)** Normalized histogram of the number of ground points in open pixels.

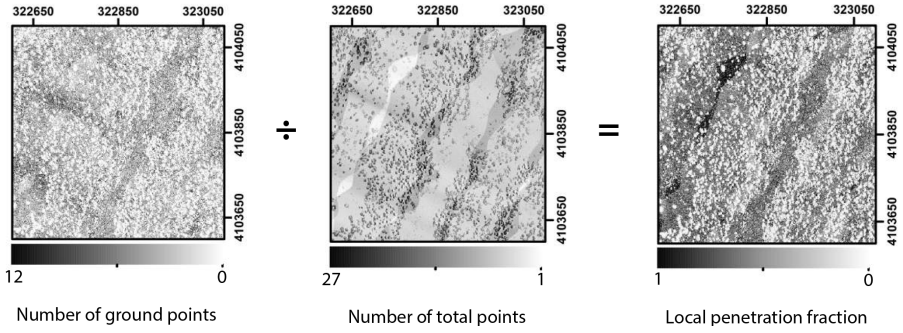

Figure 3. Illustration of producing local penetration fraction from number of ground points and number of total points from LiDAR data.

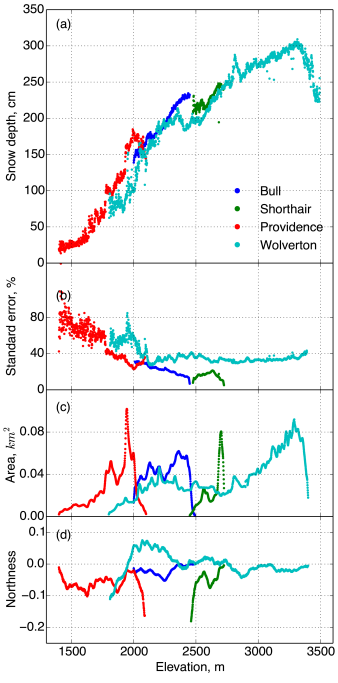

Figure 4. (a) Averaged snow depth from snow-on and snow-off LiDAR data vs. elevation in four sites. **(b)** Standard error of the snow depth within each 1 m elevation band. **(c)** Total area of averaged data within each elevation band. **(d)** Averaged northness of each elevation band from four sites.

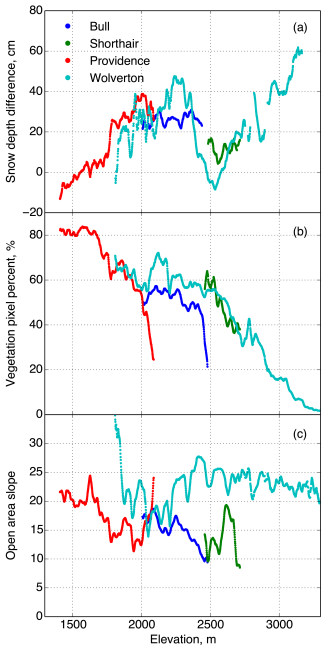

Figure 5. (a) Averaged snow-depth difference between open and vegetated area along elevation gradient in four sites. **(b)** Vegetation pixel percent of total number of pixel from canopy height model, sorted along elevation. **(c)** Averaged slope of open area along elevation gradient.

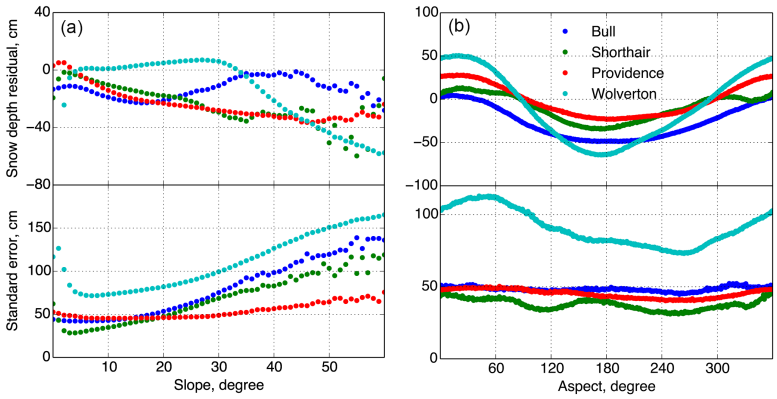

Figure 6. (a) Averaged snow-depth residual and standard deviation along slope. Raw snow-depth residual was calculated from LiDAR measured snow depth and estimated snow depth from the linear regression model. **(b)** Averaged snow-depth residual and standard deviation along aspect.

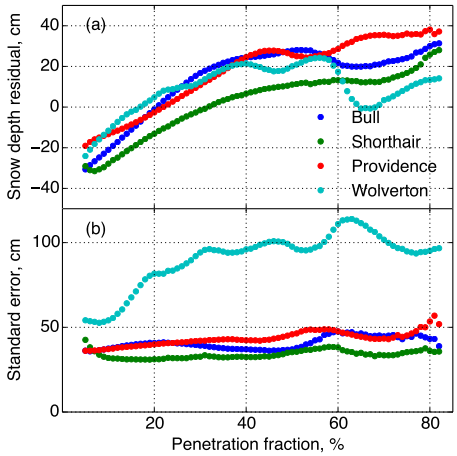

Figure 7. (a) Averaged snow-depth residual along penetration fraction. Raw snow-depth residual was calculated from LiDAR measured snow depth and estimated snow depth from the linear regression model with elevation. **(b)** Standard error of the raw snow depth residual within 1 % penetration fraction band.